Kinetics and Catalysis, Vol. 46, No. 1, 2005, pp. 77–87. Translated from Kinetika i Kataliz, Vol. 46, No. 1, 2005, pp. 85–96.

^{35}S Tracer Study of the Effect of Support Nature on the Dynamics of the Active Sites of CoMo and NiMo Sulfide Catalysts Supported on Al_2O_3 and Activated Carbon

V. M. Kogan

Zelinskii Institute of Organic Chemistry, Russian Academy of Sciences, Moscow, 119991 Russia

Received October 30, 2003

Abstract—The influence of the support (Al_2O_3 and activated carbon) on the activity of Mo, NiMo, and CoMo catalysts in thiophene hydrogenolysis is studied using ^{35}S as a tracer. The carbon-supported catalysts have more active sites than their alumina-supported counterparts, while the turnover frequencies of these sites are similar. Thiophene desulfurization and hydrogenation of the resulting C_4 olefins take place at the same Mo sites. Tracer tests have demonstrated that the active sites in the catalysts examined are identical and that the support has an effect only on their concentration.

Hydrotreating catalysts prepared by loading activated carbon with an active phase (C-supported catalysts) are more active than conventional systems based on Al_2O_3 or SiO_2 [1–9]. After the service life of a C-supported catalyst is over, metals of the active phase can be recovered by burning out the support and then reused. Furthermore, cobalt in C-supported CoMo catalysts, unlike cobalt in $CoMo/Al_2O_3$ (Al_2O_3-supported catalysts), does not react with the support to form a spinel and remains entirely in the active phase. However, there are reasons why C-supported catalysts have found only little industrial application. Firstly, although C-supported CoMo catalysts show a very high specific activity, their support has a low density and, accordingly, they are inferior to Al_2O_3-supported catalysts in terms of activity per liter (which is an industrially accepted characteristic of catalysts). Secondly, about 50% of the pore volume in activated carbon is due to micropores, which can limit the diffusion of the reactants.

These are the reasons why C-supported catalysts are primarily interesting as model systems for investigating the effect of the support on the performance of the active phase. Most studies in this field have dealt with the structure of catalysts, the effects of the preparation method and support on this structure, and the correlation between these characteristics and catalytic activity [7–13].

X-ray photoelectron spectroscopy (XPS) [14] revealed different types of interaction between the support (Al_2O_3 or activated carbon) and molybdenum sulfide as an active phase. XPS data indicate the presence of MoS_2 and cobalt sulfide species (Co_9S_8, Co–Mo–S, and $CoMo_2S_2$) in sulfided CoMo/C and $CoMo/Al_2O_3$ catalysts. However, these species are difficult to identify, because they give rise to very similar Co2*p* spectra [15]. Mössbauer emission spectroscopy and X-ray absorption spectroscopy confirmed the presence of a Co–Mo–S phase in the CoMo/C catalysts [16–20]. The fact that the active phase in C-supported catalysts is not bound to the support through oxygen atoms suggests that the Co–Mo–S species on carbon differ in properties from the same species on alumina. Two types of Co–Mo–S structure were discovered in Al_2O_3-supported catalysts [21, 22]. Type I structures form at conventional sulfiding temperatures; type II structures form at ordinary or elevated temperatures, but they require special impregnation conditions. The Co–Mo–S structures on activated carbon are type II. This fact is consistent with the assumption that type I Co–Mo–S structures are more strongly bound to the support and, therefore, less active than type II structures [23].

Owing to the strong interaction between the active phase and Al_2O_3, small molybdenum disulfide crystallites are uniformly distributed over the support surface and are stable (primarily with respect to agglomeration) during the catalytic reaction. At the same time, the strong interaction in Al_2O_3-supported catalysts is disadvantageous: it favors formation of the low-active (type I) Co–Mo–S structure.

In order to understand the principles of functioning of the active phase on different supports, it is necessary to study the transformations of organosulfur compounds on the surface of this phase. A number of recent studies have been devoted to the kinetics of conversion of thiophene and dibenzothiophenes on C-supported Co- and Ni-containing molybdenum sulfide catalysts of various compositions [24–29]. These studies have dealt with the effects of the partial pressure of hydrogen sulfide, N- containing additives in the reaction mixture and

0023-1584/05/4601-0077 © 2005 MAIK “Nauka / Interperiodica”

Table 1. Results of the tracer study of the γ-Al_2O_3- and carbon-supported molybdenum sulfide catalysts

Composition of the active phase		Υ, %	C_4H_{10}/C_4H_8	S_{stoich}, %	S_{mob}, mg	$\Pi_{fast} \times 10^2$	SH/CUS	V^*_{fast}	ES*
Mo, wt %	support								
3	Al_2O_3	7.30	0.084	2.00	0.58	5.1	2.65	51	327
6	Al_2O_3	15.54	0.134	4.00	0.87	7.2	1.20	72	764
10	Al_2O_3	23.70	0.210	6.67	1.01	9.5	0.61	95	1548
12	Al_2O_3	27.08	0.284	8.00	2.12	10.0	0.50	104	1916
3	C	8.36	0.165	2.00	0.97	3.5	0.95	35	1018
6	C	16.27	0.357	4.00	1.29	5.1	0.48	51	2051
12	C	35.70	0.491	8.00	2.33	6.2	0.41	62	2365

Note: Υ is thiophene conversion, S_{stoich} is the sulfur content of the catalyst calculated on the basis of MoS_2 stoichiometry, S_{mob} is the amount of mobile sulfur (for Mo/Al_2O_3, $S_{mob} = S_{fast}$), Π_{fast} is the turnover frequency of the active sites borne by Mo, SH/CUS is the ratio of the number of coordinatively unsaturated sites to the number of SH groups, V_{fast} is the number of functioning vacancies, and ES is the number of empty sites.

* Per 1000 SH groups.

reaction conditions. It is assumed that desulfurization and hydrogenation sites are different and that coordinatively unsaturated sites (CUS's) play a key role in hydrodesulfurization. However, the above-mentioned studies have provided no direct experimental evidence that CUS's exist. Indeed, no quantitative estimates have been reported for the properties of these sites. A tracer method [30–32] enabled us to determine the number of surface SH groups and CUS's, evaluate the reactivity of active sites, and correlate these data with the composition of the active phase of the sulfide catalyst. Here, we report a tracer investigation of the dependence of catalyst activity in thiophene hydrogenolysis on the nature of the support.

EXPERIMENTAL

We examined four series of Mo catalysts (Table 1) and CoMo and NiMo bimetallic catalysts (Table 2) supported on γ-Al_2O_3 and activated carbon. The molybdenum content of Mo/Al_2O_3 and Mo/C catalysts was varied between 3 and 12 wt %. Furthermore, we tested a series of samples containing 10% Mo, varying the Co concentration between 0.5 and 4%. The catalysts were prepared by impregnating γ-Al_2O_3 (specific surface area, 240 m^2/g; pore volume, 0.54 cm^3/g) and coconut charcoal (specific surface area, 820 m^2/g; pore volume, 0.46 cm^3/g) with aqueous solutions containing appropriate amounts of ammonium heptamolybdate and nickel (cobalt) nitrate. The impregnated materials were dried at 110°C for 2 h and calcined at 500°C for 3 h.

Prior to tracer tests, the catalysts were sulfided with elementary ^{35}S in a 21-cm^3 autoclave at P_{H_2} = 6 MPa, T = 360°C, and a catalyst-to- sulfur ratio of 5 : 1 for 1 h.

A catalyst sample containing radioactive sulfur (25–200 mg) was transferred into a pulsed catalytic microreactor coupled with a radiometric chromatograph (Fig. 1). The catalyst was treated with helium, and the hydrogen flow (chromatographic carrier gas) was switched over to pass through the reactor. This was followed by pulsed injection of 1-μl portions of unlabeled thiophene into the reactor.

The reaction yielded C_4 hydrocarbons and hydrogen sulfide. Radioactivity was detected only in hydrogen sulfide. The molar radioactivity of the resulting hydrogen sulfide gradually decreased as the number of thiophene portions injected increased, because the radioactive sulfur of the catalyst was progressively replaced by the nonradioactive sulfur of thiophene.

Chromatographic analysis of thiophene conversion products was carried out in two modes. In the first mode, the products were separated into hydrogen sulfide, hydrocarbons, and thiophene to measure the radioactivity of the hydrogen sulfide. In this mode, we used column 1 (Fig. 1), which was packed with 15% Carbowax/Celite 545 (3 mm × 3 m; 120°C). Analysis of the hydrocarbon fraction was carried out in the second mode. In this mode, after the products were separated in column 1, the hydrocarbon fraction and hydrogen sulfide were collected in trap 2 and then directed to col-

Table 2. Results of the tracer study of the γ-Al_2O_3- and carbon-supported Ni(Co)Mo sulfide catalysts

Composition of the active phase				r	ϒ, %	C_4H_{10}/C_4H_8	S_{tot}, %	S_{mob}, mg	S_{fast}, mg	S_{slow}, mg	$\Pi_{fast} \times 10^2$	$\Pi_{slow} \times 10^2$	SH/CUS	V^*_{fast}	V^*_{slow}	ES*
Mo, wt %	Ni, wt %	Co, wt %	support													
6.8	0	0	Al_2O_3	0	11.9	0.14	4.52	0.91	0.91	0	5.3	0	1.00	53	0	943
6.8	0.9	0	Al_2O_3	0.18	45.7	0.33	5.02	1.80	0.77	1.03	18.7	4.0	8.65	80	23	36
6.8	1.8	0	Al_2O_3	0.30	49.5	0.38	5.50	1.93	0.90	1.03	16.8	4.7	7.26	79	25	59
6.8	3.5	0	Al_2O_3	0.45	58.8	0.27	6.40	2.35	0.64	1.71	20.4	6.3	11.25	56	45	33
6.8	0	0	C	0	32.6	0.37	4.53	2.24	2.24	0	5.9	0.0	0.98	59	0	962
6.8	0.9	0	C	0.18	76.6	0.98	5.04	2.45	1.41	1.04	18.7	4.5	0.94	108	19	951
6.8	1.8	0	C	0.30	80.7	1.24	5.51	2.30	1.25	1.04	21.5	5.6	0.71	117	25	1283
6.8	3.5	0	C	0.46	79.4	1.30	6.43	2.85	0.93	1.93	19.1	7.5	0.80	62	51	1191
10	0	0	Al_2O_3	0	23.7	0.21	6.67	1.01	1.01	0	9.5	0	0.61	95	0	1548
10	0	0.5	Al_2O_3	0.08	56.2	0.27	6.94	2.17	0.82	1.35	22.3	3.4	3.55	94	11	197
10	0	1	Al_2O_3	0.14	71.8	0.26	7.21	2.08	0.66	1.41	26.5	8.2	2.58	105	36	303
10	0	1.5	Al_2O_3	0.20	80.9	0.36	7.48	2.37	0.56	1.81	31.9	8.3	3.79	115	23	188
10	0	3	Al_2O_3	0.33	90.7	0.35	8.29	2.76	0.53	2.23	56.7	3.1	4.94	108	25	94
10	0	4	Al_2O_3	0.39	83.6	0.28	8.84	2.96	0.39	2.57	67.0	2.9	5.18	89	25	104
10	0	0.5	C	0.08	53.5	0.40	6.94	2.35	0.81	1.54	18.9	4.2	0.51	65	27	1884
10	0	1	C	0.14	52.2	0.75	7.21	2.71	0.74	1.97	23.6	6.0	0.60	74	34	1596
10	0	1.5	C	0.20	89.9	1.96	7.48	3.15	0.62	2.53	42.1	4.1	0.73	93	23	1290
10	0	3	C	0.33	93.4	5.89	8.29	3.64	0.57	3.07	52.5	2.6	0.78	82	22	1195
10	0	4	C	0.39	89.8	5.61	8.84	3.95	0.45	3.50	63.8	2.2	0.81	73	19	1164

Note: Experimental conditions: catalyst weight, 100 mg; T = 360°C; hydrogen flow rate, 20 cm^3/min; thiophene injected per pulse, 1 μl.
* Per 1000 SH groups.

umn 2 (12% tributyl phosphate/Chromosorb P; 3 mm × 7.5 m; 25°C).

Signals from the thermal-conductivity detector and radiation counter were processed in the on-line mode using the Mul'tikhrom 2.74 program. The radioactivity of hydrogen sulfide was measured with a flow- type proportional radiation counter. The quencher was methane, which was fed into the counter as a 1 : 1 mixture with the carrier gas. The sulfur content of ^{35}S-labeled catalyst samples was determined by measuring their specific radioactivity (SR) and comparing it with the SR of the sulfiding agent. Processing of experimental data is described elsewhere [31].

RESULTS AND DISCUSSION

Unpromoted Catalysts MoS_2/Al_2O_3 and MoS_2/C

Experimental data for the MoS_2/Al_2O_3 and MoS_2/C catalysts are presented in Table 1 and Figs. 2–7. It is clear from Fig. 2 that the concentration of mobile sulfur, S_{mob}, and its fraction in the total amount of sulfide sulfur are much greater in the C-supported catalysts than in the Al_2O_3-supported catalysts. Therefore, both the S_{mob} content and the ratio of surface (mobile) sulfur to bulk (immobile) sulfur depend on the nature of the support.

In the C-supported catalysts, as in MoS_2/Al_2O_3, the proportion of mobile sulfur decreases as the Mo content is raised. A plausible explanation of this fact is that

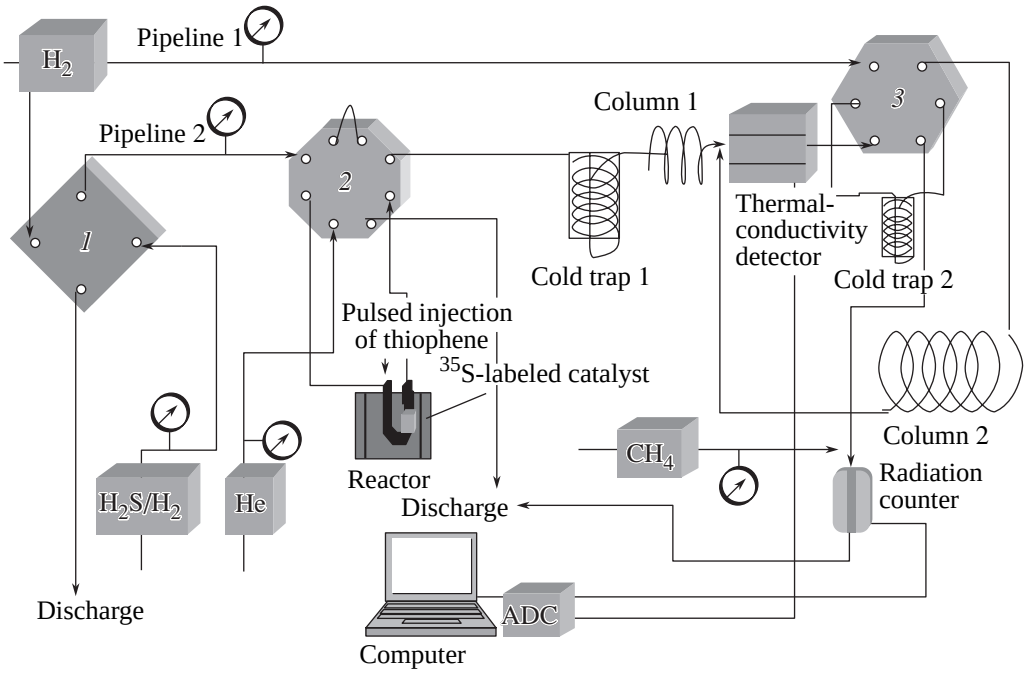

Fig. 1. Schematic of the pulsed catalytic setup, including on-line radiochromatographic analysis of the products: (*1*) four-way valve, (*2*) eight-way valve, and (*3*) six-way valve; ADC is an analog-to-digital converter.

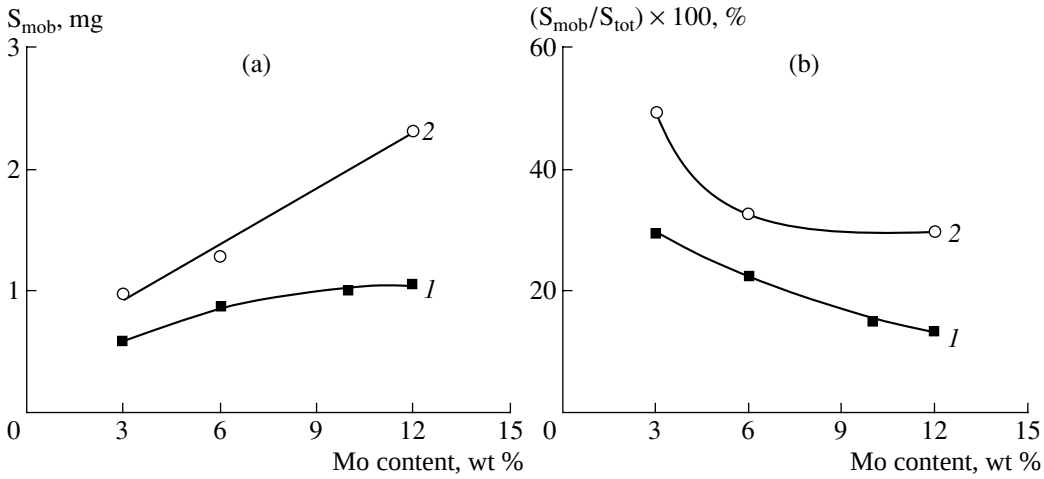

Fig. 2. (a) Amount and (b) fraction of mobile sulfur as a function of Mo content for (*1*) alumina- and (*2*) carbon-supported molybdenum sulfide catalysts.

the molybdenum sulfide phase coarsens with increasing Mo content of the catalyst. However, the shape of the mobile- sulfur curve is support dependent. For MoS_2/Al_2O_3, S_{mob}/S_{tot} decreases monotonically. For MoS_2/C, this ratio falls markedly between 3 and 6% Mo, while further raising of the Mo content does not cause considerable changes in S_{mob} and, accordingly, molybdenum sulfide particle size.

Furthermore, raising the Mo content reduces the SH/CUS ratio (Fig. 3), and the proportion of SH groups decreases much more rapidly in MoS_2/Al_2O_3 than in Mo/C. Comparing the curves plotted in Figs. 2b and 3 suggests that SH/CUS and S_{mob}/S_{tot} vary in the same way and that the amount of CUS's in the unpromoted Al_2O_3- and C-supported molybdenum catalysts is proportional to S_{tot} content (Fig. 4).

In our earlier studies [30, 31], we arrived at the conclusion that CUS's are a totality of functioning vacancies (Vs) and empty sites (ES's): $\Sigma CUS = \Sigma V + \Sigma ES$. Comparison between Figs. 5a and 5b demonstrates that the relative amounts of Vs and ES's increase in proportion to Mo content.

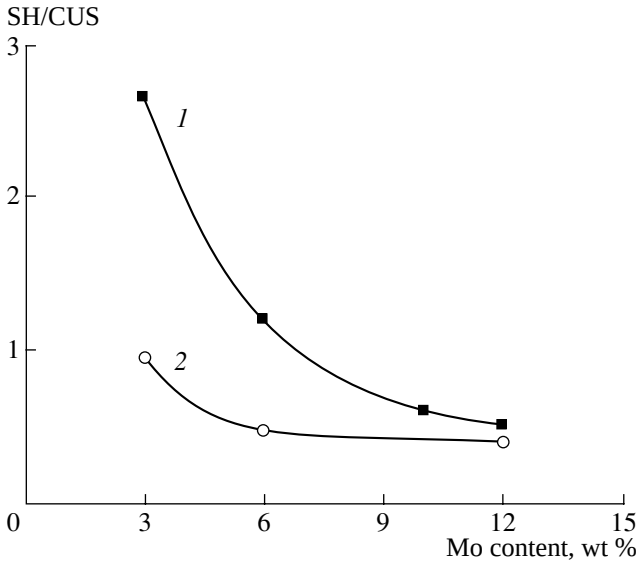

Fig. 3. SH/CUS as a function of Mo content for the (*1*) MoS_2/Al_2O_3 and (*2*) MoS_2/C catalysts.

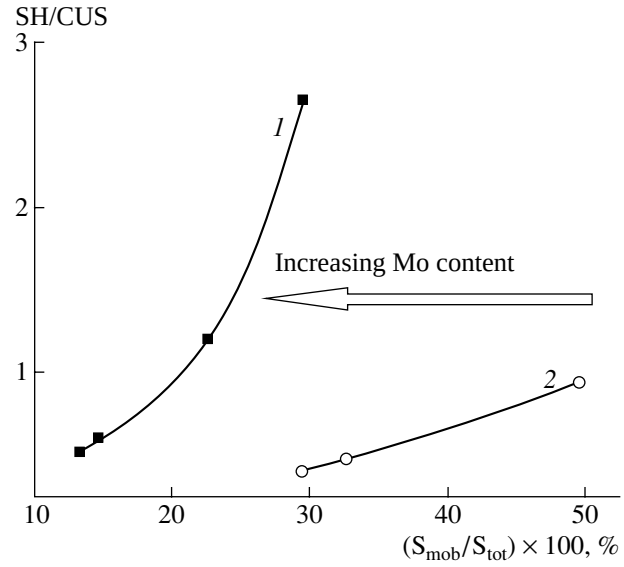

Fig. 4. SH/CUS as a function of S_{mob}/S_{tot} for the (*1*) MoS_2/Al_2O_3 and (*2*) MoS_2/C catalysts with different Mo contents.

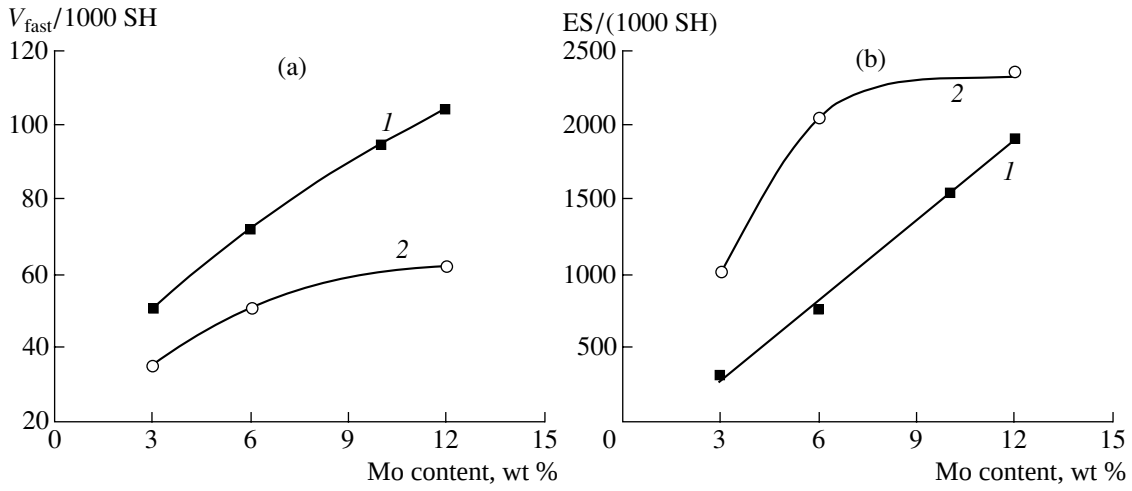

Fig. 5 (a) V and (b) ES densities as a function of Mo content for the (*1*) MoS_2/Al_2O_3 and (*2*) MoS_2/C catalysts.

Analysis of these data together with the evaluated catalytic activity data for thiophene hydrodesulfurization (Fig. 6) shows that the specific activity of the molybdenum catalyst depends only slightly on the support and the amount of the active phase. Therefore, by changing the support or varying the amount of the active phase, one can change only the number of active sites, not their activity.

Figure 7 shows how the butane : butenes ratio, which is a characteristic of hydrogenating capacity, depends on the density of functioning vacancies (number of Vs per 1000 SH groups) for the $MoS_2/Al_2O_3$and MoS_2/C catalysts. The hydrogenating capacity of these catalysts, like that of catalysts poisoned with N-containing compounds [32], depends linearly on the density of the vacancies responsible for desulfurization. This finding confirms the deduction that thiophene hydrogenation and desulfurization take place at the same sites.

As compared to the MoS_2/Al_2O_3 catalysts, the MoS_2/C catalysts have a higher hydrogenating capacity, which is attainable at a lower V density. This is due to the fact that the C-supported catalysts have more mobile sulfur (surface SH groups) than the Al_2O_3-supported catalysts (apparently because the active phase in the former is more finely dispersed). Therefore, the

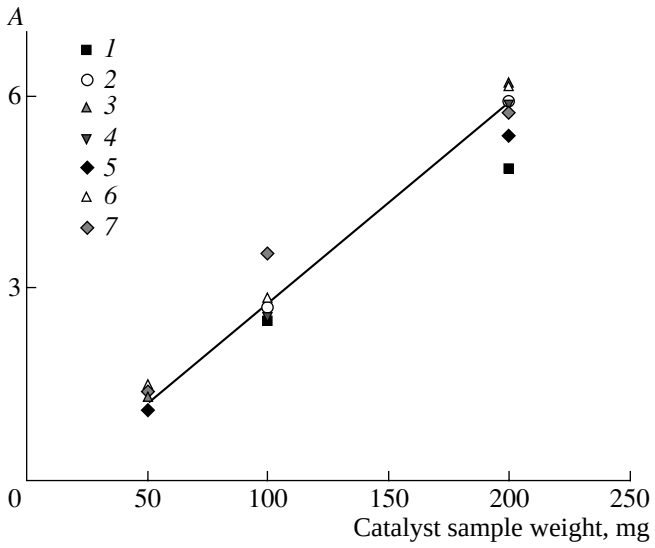

Fig. 6. Specific catalytic activity $A = -\ln(1 - \gamma)$/Mo as a function of the catalyst sample weight for the (*1–4*) alumina- and (*5–7*) carbon-supported molybdenum catalysts containing (*1*, *5*) 3, (*2*, *6*) 6, (*3*) 10, and (*4*, *7*) 12% Mo. γ is thiophene conversion.

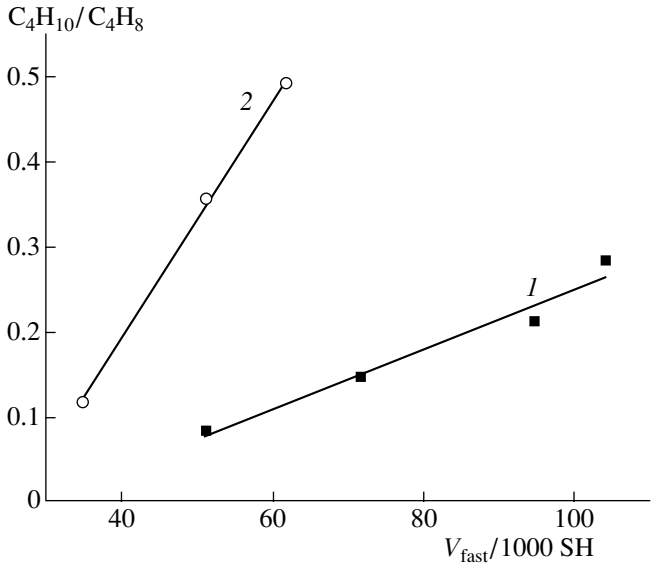

Fig. 7. Hydrogenating capacity (C_4H_{10}/C_4H_8) as a function of V density (V_{fast}/(1000 SH)) for unpromoted (*1*) MoS_2/Al_2O_3 and (*2*) MoS_2/C with different Mo contents.

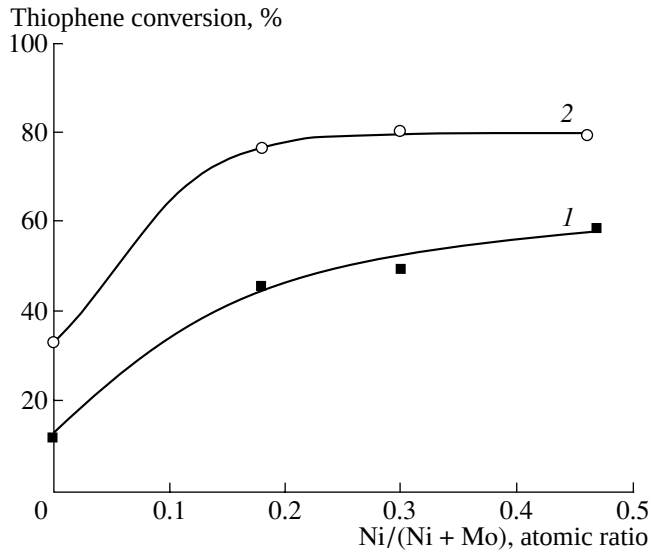

Fig. 8. Thiophene conversion as a function of promoter content for the (*1*) Al_2O_3- and (*2*) C-supported NiMo sulfide catalysts.

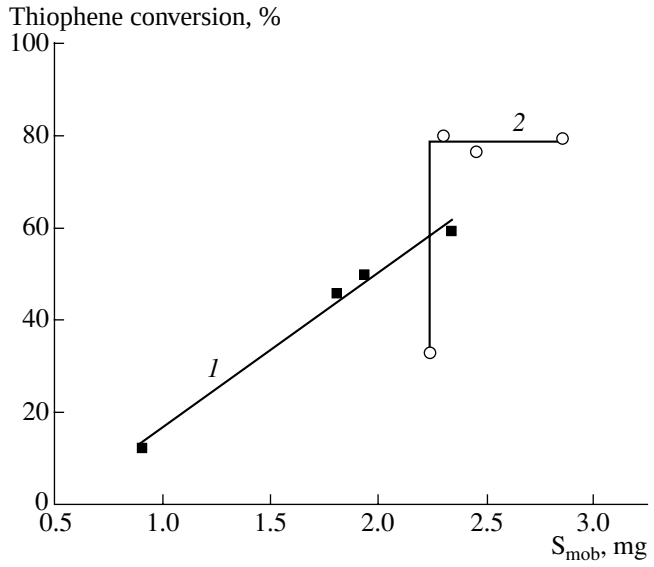

Fig. 9. Thiophene conversion as a function of the amount of mobile sulfur for the (*1*) Al_2O_3- and (*2*) C-supported NiMo sulfide catalysts.

fraction of Vs per SH group in the C-supported catalysts is lower than this fraction in the Al_2O_3-supported catalysts. The total number of vacancies per Mo atom in the C-supported catalysts is somewhat higher than that in the Al_2O_3-supported catalysts. These results are in good agreement with earlier data suggesting the existence of two types of MoS_2 phase [23, 33], as in the case of the Co(Ni)–Mo–S phase. According to those data, type I MoS_2 phase dominates in catalysts with low Mo content and interacts strongly with the support. Type II MoS_2 phase forms in catalysts that are rich in Mo and/or are supported on an inert material.

NiMo and CoMo Promoted Catalysts Supported on Al_2O_3 and Activated Carbon

These catalysts are similar to the unpromoted catalysts in that they are sulfided to the maximum possible sulfur content corresponding to the formation of sto-

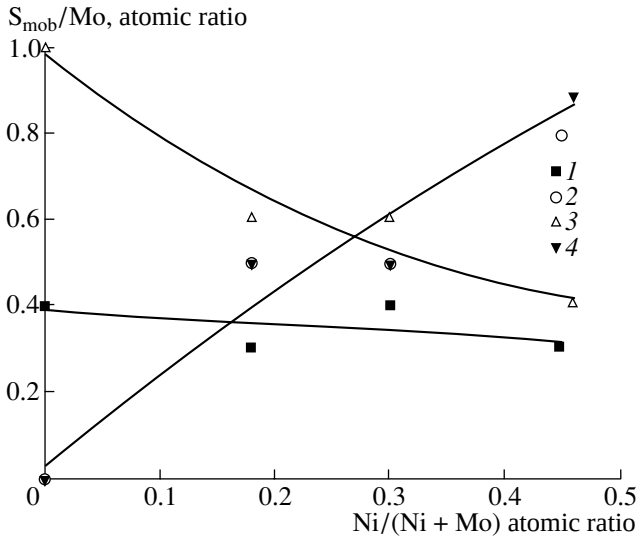

Fig. 10. Mobile sulfur per gram-atom of Mo as a function of promoter content for the (*1*, *3*) fast and (*2*, *4*) slow active sites of the (*1*, *2*) Al_2O_3- and (*3*, *4*) C-supported NiMo sulfide catalysts.

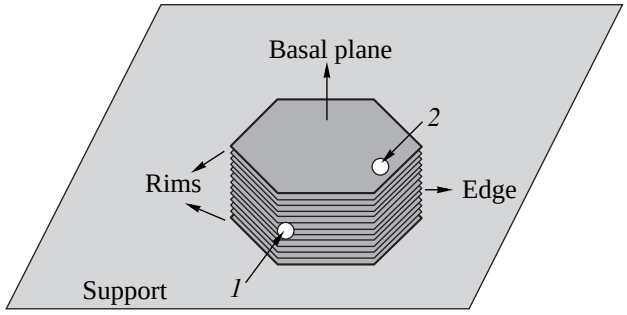

Fig. 11. Edge–rim model of the active phase of the MoS_2 catalyst [29]. The white circles are possible thiophene adsorption sites on the (*1*) edge and (*2*) basal plane.

ichiometric MoS_2 and NiS in the active phase. It follows from the data presented in Table 2 and Fig. 8 that the NiMoS/C catalysts are much more active in both desulfurization and hydrogenation than their Al_2O_3-supported counterparts of the same composition.

Introducing a promoter (Ni) produces different effects on catalyst activity and the ratio between conversion and the amount of mobile sulfur: for the Al_2O_3-supported catalysts, these quantities are linearly interrelated; for the C-supported catalysts, even small amounts of the promoter cause a drastic rise in catalytic activity. In the latter case, promoter concentration has only a minor effect on the mobile-sulfur content, and further raising the latter does not increase the catalytic activity (Fig. 9). The unusual shape of the conversion versus mobile sulfur curve for the C-supported catalysts, particularly striking as compared with the linear dependence for the Al_2O_3-supported catalysts, apparently indicates that introduction of Ni causes qualitative changes in the active phase of the C-supported catalysts. Possible changes of this kind are alteration of the nature of active centers and redistribution of active centers caused by changes in the particle size of the active phase. It is, therefore, pertinent to make a more thorough analysis of data relevant to the mobility and distribution of mobile sulfur in the active phase.

It was demonstrated [31] that the active phase of the $CoMo/Al_2O_3$ and $NiMo/Al_2O_3$ bimetallic catalysts has two types of surface SH group differing in capacity for forming H_2S (mobility) and, accordingly, two types of active site (AS) differing in reactivity. The more reactive sites (fast AS's) are associated with Mo, and the less reactive sites (slow AS's) are associated with Co.

Figure 10 plots S_{mob}/Mo as a function of the promoter content r = Ni/(Ni + Mo) for the γ-Al_2O_3- and C-supported catalysts. For unpromoted MoS_2/Al_2O_3, $S_{mob}/Mo = 0.4$. The S_{tot}/Mo ratio in this catalyst is about 2; that is, 1/5 of the total sulfide sulfur participates in hydrogen sulfide formation. This result supports the assumption that reactive sulfur is the sulfur located on the edges of MoS_2 crystallites. The sulfide sulfur of the basal planes of alumina-supported MoS_2 crystallites is inactive. For the MoS_2/C catalyst, $S_{mob}/Mo \approx 1$, while the S/Mo ratio in molybdenum disulfide is 2. Therefore, mobile sulfur makes up only half of the total sulfide sulfur. From this, we inferred that active sulfur in MoS_2 clusters is located not only on crystallite edges but also in basal planes, probably near the crystallite edges [34]. Those regions were called rims [35] (Fig. 11).

It was demonstrated by EXAFS that there is loosely bonded sulfur in the basal plane of molybdenum disulfide crystallites, and it was assumed that this plane can adsorb thiophene [36].

This assumption has recently received indirect support [37]. The interaction between thiophene and flat molybdenum disulfide crystallites on a neutral (gold) support (MoS_2/Au) was studied by scanning tunneling microscopy, and it was found that thiophene is adsorbed near edges of the basal planes of MoS_2 crystallites. Thiophene is activated owing to hydrogenation of the C=C bond followed by cleavage of the C–S bond. Obviously, this pathway of the reaction is, to a considerable extent, due to the inertness of the support and the weakness of the support–active phase interaction. Similar processes are possible on the basal planes of C-supported molybdenum disulfide, since MoS_2-support interaction may be weak because of the inertness of carbon.

The fact that the number of fast sites in the NiMo catalysts grows with increasing promoter content is in agreement with the shape of the corresponding curve for fast sites in the CoMo catalysts (see above). Comparing the curves for the Al_2O_3- and C-supported catalysts (Fig. 10) demonstrates that, as the Ni content is

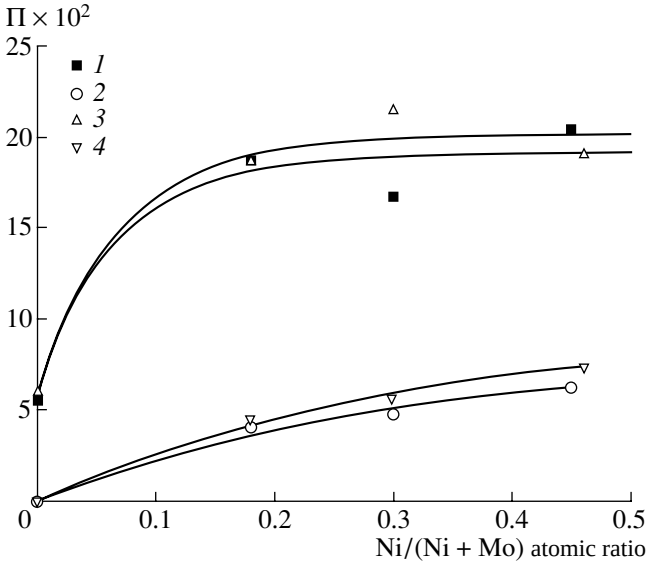

Fig. 12. Turnover frequency Π of the (*1*, *3*) fast and (*2*, *4*) slow active sites as a function of promoter content for the (*1*, *2*) Al_2O_3- and (*3*, *4*) C-supported promoted NiMo sulfide catalysts (6.8 wt % Mo).

increased, the number of fast AS's in the C-supported catalysts decreases markedly, while this characteristic of the Al_2O_3-supported catalysts changes little. The point is that the AS's in basal planes of Al_2O_3-supported MoS_2 crystallites are inactive (Fig. 11). Therefore, the deposition of nickel sulfide particles on the basal planes of $NiMo/Al_2O_3$ crystallites does not change the number of mobile SH groups bound to fast AS's. For the C-supported catalysts, blocking of basal and edge sites results in a more rapid descent of the fast-AS curve. Raising the Ni content increases the number of slow sites in the Al_2O_3- and C-supported catalysts at equal rates (the corresponding curves coincide). Therefore, catalytic activity is shown only by nickel sulfide particles situated on the edges of MoS_2 crystallites, while the particles blocking active MoS_2 sites in the basal planes do not form "slow" sites capable of participating in hydrogen sulfide formation.

These results are consistent with turnover frequency data as a function of promoter content (Fig. 12). For the unpromoted MoS_2/Al_2O_3 and MoS_2/C catalysts, 0.05 molecules of hydrogen sulfide are formed and the same number of thiophene molecules are converted per pulse at one SH group. Therefore, every 20th (1/0.05) group takes part in hydrogen sulfide formation. These SH groups are fast sites borne by Mo. Introducing a promoter brings about slow active sites. The turnover frequency of both types of site increases with increasing Ni content of the active phase. At $r = 0.45$, the turnover frequency of the fast sites is $\Pi_{fast} \approx 0.2$: every fifth SH group belonging to the fast sites participates in H_2S formation. For slow sites, $\Pi_{slow} \approx 0.06$ at the same r, indicating that one of 16 SH groups of this type is involved in the reaction.

Coincidence of turnover frequency versus promoter content curves for one type of AS and different supports (Al_2O_3 and carbon) is also observed for the CoMo catalysts (Fig. 13). Therefore, only the number of AS's, not their nature and properties, depend on the support. Indeed, the NiMo/C catalysts have a larger number of fast AS's than the Al_2O_3-supported catalysts of the

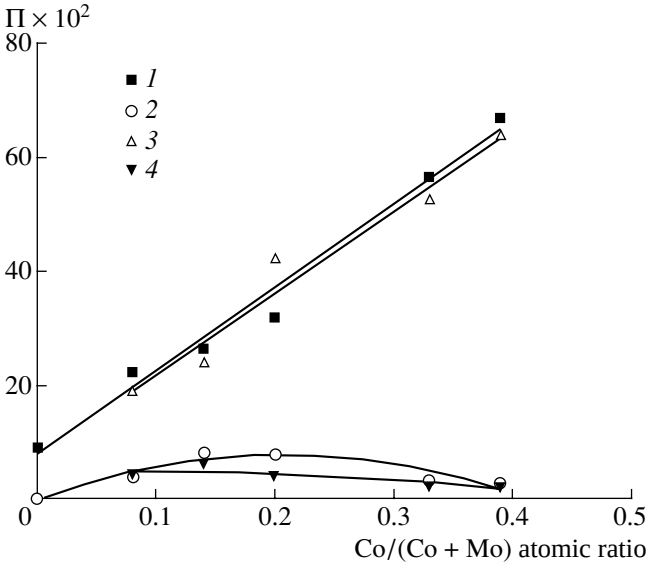

Fig. 13. Turnover frequency Π of the (*1*, *3*) fast and (*2*, *4*) slow active sites as a function of promoter content for the (*1*, *2*) Al_2O_3- and (*3*, *4*) C-supported promoted CoMo sulfide catalysts (10 wt % Mo).

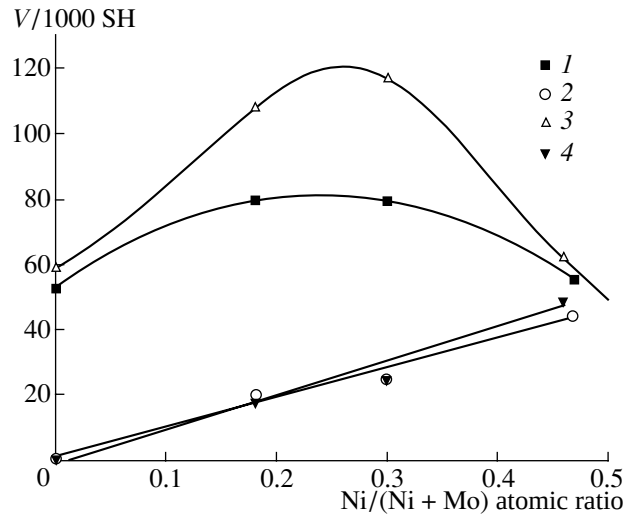

Fig. 14. Density of (*1*, *3*) fast and (*2*, *4*) functioning vacancies (*V*) as a function of promoter content for the (*1*, *2*) $NiMo/Al_2O_3$ and (*3*, *4*) NiMo/C sulfide catalysts.

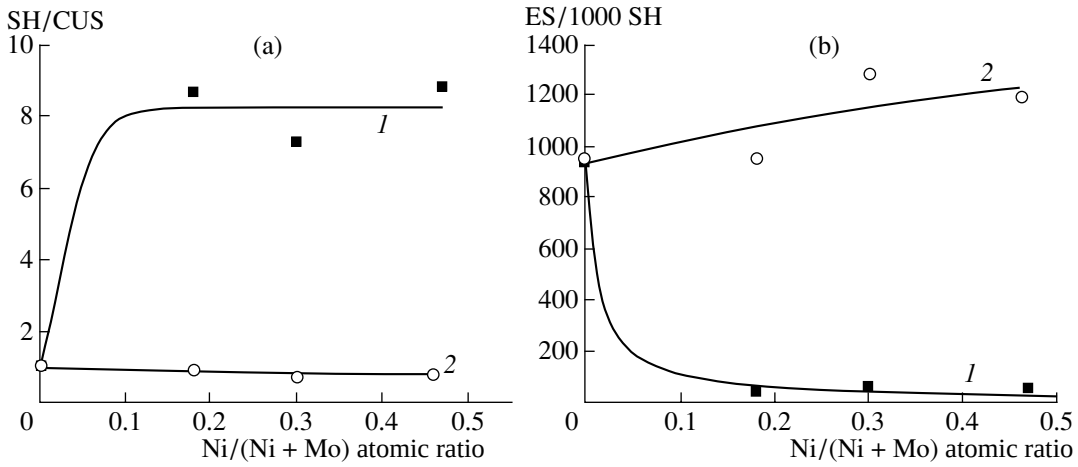

Fig. 15. (a) SH/CUS and (b) ES/(1000 SH) as a function of promoter content for the (*1*) NiMo/Al_2O_3 and (*2*) NiMo/C sulfide catalysts.

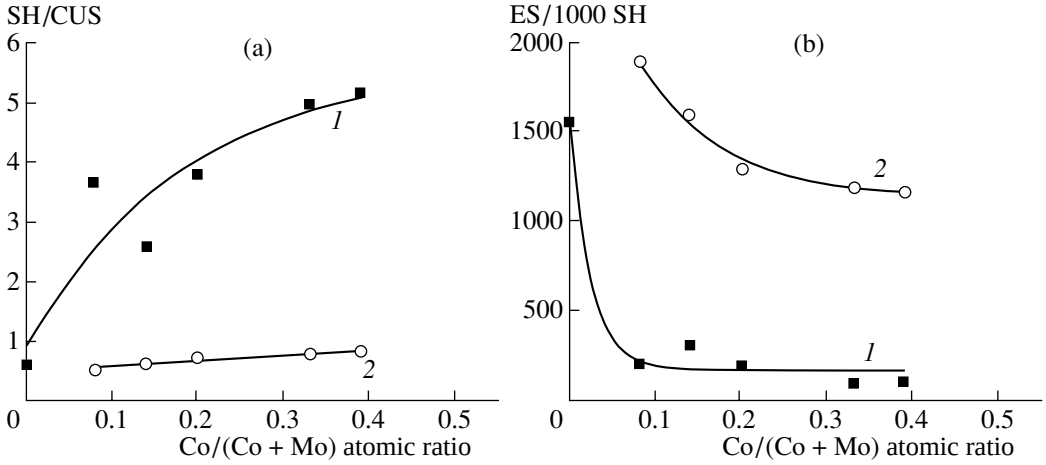

Fig. 16. (a) SH/CUS and (b) ES/(1000 SH) as a function of promoter content for the (*1*) CoMo/Al_2O_3 and (*2*) CoMo/C sulfide catalysts.

same composition. The number of slow sites is support-independent and is determined by the amount of promoter introduced. This is particularly clear from the promoter-content dependence of the ratio of the number of Vs to the number of SH groups for fast and slow AS's in the Al_2O_3- and C-supported catalysts (Fig. 14). The C-supported catalysts far exceed their Al_2O_3-supported counterparts in terms of the relative number of vacancies. Both of the fast-vacancy density (V_{fast}) curves have a maximum near $r = 0.3$; that is, V_{fast} peaks near the region of the NiMoS phase. The slow-vacancy density (V_{slow}) curves for the Al_2O_3- and C-supported catalysts almost coincide and ascend slowly with increasing r. Analysis of data presented in Figs. 12–14, and 15a demonstrates that, in the promoted MoS_2 catalysts, the ratio of the number of surface SH groups to the number of CUS's, as well as the ratios between the number of Vs, the number of ES's, and the number of SH groups, are all almost independent of support nature. Introducing a small amount of Ni into the MoS_2/Al_2O_3 catalyst causes a dramatic increase in the SH coverage of surface of the active phase (Fig. 15a) owing to the decreasing number of ES's (Fig. 15b).

This trend is shown by both N- and Co-promoted catalysts supported on Al_2O_3 (Figs. 15a, 16a). In the C-supported catalysts, the proportion of CUS's varies little with promoter content because of the gradual variation in the fraction of empty sites (Figs. 15b, 16b). This insignificant effect of the promoters on the number of CUS's is apparently due to the fact that the support and the active phase in the C-supported catalysts interact weakly, irrespective of whether a promoter is present. As a consequence, the C-supported catalysts have a lower SH coverage of active-phase surface and a larger fraction of ES's than the Al_2O_3-supported catalysts.

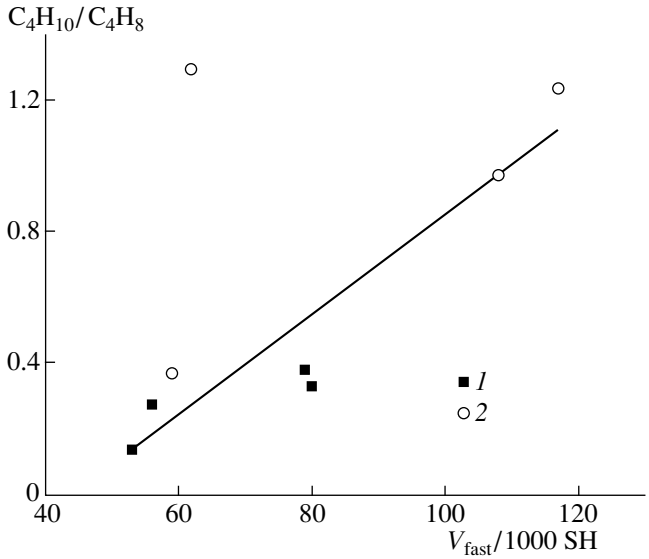

Fig. 17. Hydrogenating capacity (C_4H_{10}/C_4H_8 ratio in the thiophene hydrogenolysis product) as a function of V density (V_{fast}/(1000 SH)) for the (*1*) NiMo/Al_2O_3 and (*2*) NiMo/C sulfide catalysts.

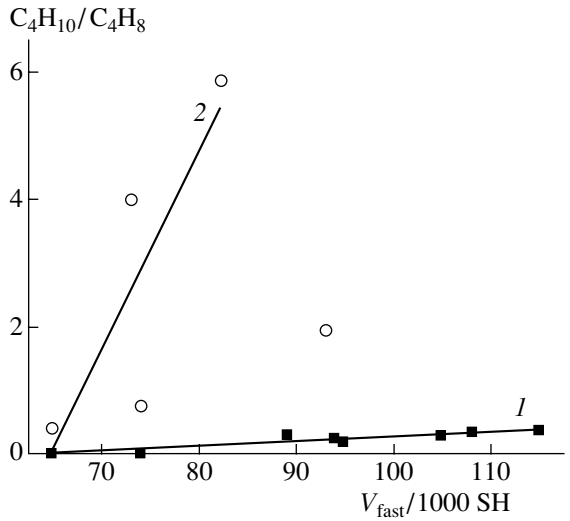

Fig. 18. Hydrogenating capacity (C_4H_{10}/C_4H_8 ratio in the thiophene hydrogenolysis product) as a function of V density (V_{fast}/(1000 SH)) for the (*1*) CoMo/Al_2O_3 and (*2*) CoMo/C sulfide catalysts.

The hydrogenation activity of the C-supported Mo and NiMo catalysts is higher than that of their Al_2O_3-supported counterparts (Table 2). The linear dependence of the hydrogenation activity of the catalyst (C_4H_{10}/C_4H_8) on the density of fast Vs (V_{fast}/(1000 SH)) (Fig. 17) suggests that both the hydrogenating and desulfurizing properties of the active sites are determined only by the number of these sites and are support-independent.

The hydrogenation activity of the CoMoS phase, unlike that of the NiMo catalysts, is support-dependent, as in the case of the unpromoted MoS_2/Al_2O_3 and MoS_2/C catalysts (Fig. 7). As is clear from Figs. 17 and 18, the C-supported CoMoS catalysts exceed the Al_2O_3- supported ones in amount of mobile sulfur (number of surface SH groups). Therefore, the number of fast Vs (V_{fast}) per SH group is smaller in the C-supported catalysts than in the Al_2O_3-supported catalysts. However, the total number of Vs in the C-supported catalysts is 3–5 times higher than that in their Al_2O_3-supported counterparts with the same composition of the active phase (see the SH/CUS data in Table 2).

In other terms, the NiMoS phase forms on both carbon and alumina and is apparently a type II phase. The CoMoS phase on carbon is always type II. The CoMoS phase on alumina can be either type I or type II, depending on the catalyst composition, preparation conditions, and the properties of the support.

CONCLUSIONS

The main results from the comparative study of the alumina and carbon-supported Mo and Ni(Co)Mo sulfide catalysts are the following:

(1) The C-supported catalysts contain more mobile sulfur than the Al_2O_3-supported catalysts because of the smaller particle size of the active phase.

(2) The SH/CUS ratio in the C-supported catalysts is much smaller than that in the Al_2O_3-supported catalysts, suggesting that the active phase in the former is reduced to a greater extent. Raising the Mo content reduces SH/CUS in both the Al_2O_3- and C-supported catalysts.

(3) The Al_2O_3- and C-supported catalysts are similar in terms of the turnover frequency of the active sites. Therefore, these sites are of the same nature. The turnover frequency of the active sites depends on the promoter content of the active phase and is support-independent.

(4) The dynamic properties of the active sites in the NiMo and CoMo catalysts are similar.

(5) The hydrogenation of butenes that have resulted from thiophene hydrogenolysis takes place on sites that are associated with Mo and responsible for desulfurization.

REFERENCES

1. De Beer, V.H.J., Duchet, J.C., and Prins, R., *J. Catal.*, 1981, vol. 72, p. 369.
2. Duchet, J.C., van Oers, E.M., de Beer, V.H.J., and Prins, R., *J. Catal.*, 1983, vol. 80, p. 386.
3. Scheffer, B., Arnoldy, P., and Moulijn, J.A., *J. Catal.*, 1988, vol. 112, p. 516.

4. Farag, H., Mochida, I., and Sakanishi, K., *Appl. Catal., A*, 2000, vol. 194, p. 147.
5. Hillerova, E., Vit, Z., and Zdrazil, M., *Appl. Catal.*, 1991, vol. 67, p. 231.
6. Farag, H., Whitehurst, D.D., Sakanishi, K., and Mochida, I., *Catal. Today*, 1999, vol. 50, p. 9.
7. Bouwens, S.M.A.M., van Zon, F.B.M., van Dijk, M.P., van der Kraan, A.M., de Beer, V.H.J., van Veen, J.A.R., and Koningsberger, D.C., *J. Catal.*, 1994, vol. 146, p. 375.
8. Laine, J., Labady, M., Severino, F., and Yunes, S., *J. Catal.*, 1997, vol. 166, p. 384.
9. Severino, F., Laine, J., and Lopez-Agudo, A., *J. Catal.*, 2004, vol. 188, p. 244.
10. Visser, J.P.R., de Beer, V.H.J., and Prins, R., *J. Chem. Soc., Faraday Trans.*, 1987, vol. 1, no. 83, p. 277.
11. Visser, J.P.R., Scheffer, B., de Beer, V.H.J., Moulijn, J.A., and Prins, R., *J. Catal.*, 1987, vol. 105, p. 277.
12. Bouwens, S.M.A.M., Koningsberger, D.C., de Beer, V.H.J., and Prins, R., *Bull. Soc. Chim. Belg.*, 1987, vol. 96, p. 951.
13. Crajé, M.W.J., *Ph. Doctoral Thesis*, Delft: University of Technology, 1992.
14. Muralidhar, G., Concha, B.E., Bartholomew, G.L., and Bartholomew, C.H., *J. Catal.*, 1984, vol. 89, p. 274.
15. Alstrup, I., Chorkendorff, I., Candia, R., Clausen, B.S., and Topsøe, H., *J. Catal.*, 1982, vol. 77, p. 397.
16. Bouwens, S.M.A.M., Koningsberger, D.C., de Beer, V.H.J., and Prins, R., *J. Phys. Chem.*, 1991, vol. 95, p. 123.
17. Van der Kraan, A.M., Craje, M.W.J., Gerkema, E., Ramselaar, W.L.T.M., and de Beer, V.H.J., *Appl. Catal.*, 1988, vol. 39, p. 7.
18. Crajé, M.W.J., Louwers, S.P.A., de Beer, V.H.J., Prins, R., and van der Kraan, A.M., *J. Phys. Chem.*, 1992, vol. 95, p. 5445.
19. Breysse, M., Bennett, B.A., Chadwick, D., and Vrinat, M., *Bull. Soc. Chim. Belg.*, 1981, vol. 90, p. 1271.
20. Crajé, M.W.J., de Beer, V.H.J., and van der Kraan, A.M., *Bull. Soc. Chim. Belg.*, 1991, vol. 108, p. 953.
21. Topsøe, H. and Clausen, B.S., *Catal. Rev.—Sci. Eng.*, 1984, vol. 26, p. 395.
22. Topsøe, H. and Clausen, B.S., *Appl. Catal.*, 1986, vol. 25, p. 273.
23. Candia, R., Villadsen, J., Topsøe, N.-Y., Clausen, B.S., and Topsøe, H., *Bull. Soc. Chim. Belg.*, 1984, vol. 93, p. 763.
24. Pawelec, B., Mariscal, R., Fierro, J.L.G., Greenwood, A., and Vasudevan, P.T., *Appl. Catal., A*, 2001, vol. 206, p. 295.
25. Hensen, E.J.M., Brans, H.J.A., Lardinois, G.M.H.J., de Beer, V.H.J., van Veen, J.A.R., and van Santen, R.A., *J. Catal.*, 2000, vol. 192, p. 98.
26. Sakanishi, K., Nagamatsu, T., Mochida, I., and Duayne Whitehurst, D., *J. Mol. Catal. A: Chem.*, 2000, vol. 155, p. 101.
27. Ferrari, M., Maggi, R., Delmon, B., and Grange, P., *J. Catal.*, 2001, vol. 198, p. 47.
28. Farag, H., Mochida, I., and Sakanishi, K., *Appl. Catal., A*, 2000, vols. 194–195, p. 147.
29. Lee, J.J., Han, S., Kim, H., Koh, J.H., Hyeon, T., and Moon, S.H., *Catal. Today*, 2003, vol. 86, p. 141.
30. Kogan, V.M., Rozhdestvenskaya, N.N., and Korshevets, I.K., *Appl. Catal., A*, 2002, vol. 234, p. 207.
31. Kogan, V.M., Parfenova, N.M., Gaziev, R.G., Rozhdestvenskaya, N.N., and Korshevets, I.K., *Kinet. Katal.*, 2003, vol. 44, no. 4, p. 638.
32. Kogan, V.M., Gaziev, R.G., Lee, S.W., and Rozhdestvenskaya, N.N., *Appl. Catal., A*, 2003, vol. 251, p. 187.
33. Miciukiewicz, J. and Massoth, F.E., *J. Catal.*, 1989, vol. 119, p. 531.
34. Kogan, V.M., Thi Dung Nguen, and Yakerson, V.I., *Bull. Soc. Chim. Belg.*, 1995, vol. 104, p. 303.
35. Daage, M. and Chianelli, R.R., *J. Catal.*, 1994, vol. 149, p. 414.
36. Kochubey, D.I. and Babenko, V.P., *React. Kinet. Catal. Lett.*, 2002, vol. 77, no. 2, p. 237.
37. Lauritsen, J.V., Nyberg, M., Vang, R.T., Bollinger, M.V., Clausen, B.S., Topsøe, H., Jacobsen, K.W., Lægsgaard, E., Norskov, J.K., and Besenbacher, F., *Nanotechnology*, 2003, vol. 14, p. 385.